Journal of Cellular Biochemistry 97:999–1016 (2006)

PLP1 Alternative Splicing in Differentiating Oligodendrocytes: Characterization of an Exonic Splicing Enhancer

Erming Wang,[1] Zhong Huang,[2] Grace M. Hobson,[3,4] Neviana Dimova,[1] Karen Sperle,[3] Andrew McCullough,[5] and Franca Cambi[1]*

[1]Department of Neurology, University of Kentucky, Lexington, Kentucky
[2]Department of Biochemistry and Molecular Pharmacology, Thomas Jefferson University, Philadelphia, Pennsylvania
[3]Nemours Biomedical Research, Alfred I. duPont Hospital for Children, Nemours Children's Clinic—Wilmington, Wilmington, Delaware
[4]Department of Pediatrics, Thomas Jefferson University, Philadelphia, Pennsylvania
[5]Baylor College of Medicine, Houston, Texas

Abstract Proteolipid protein (PLP) and DM20 are generated by alternative splicing of exon 3B of *PLP1* transcript in differentiating oligodendrocytes. We investigated the role of exonic splicing enhancers (ESE) in the selection of PLP 5′ donor site, focusing on putative ASF/SF2, and SC35 binding motifs in exon 3B on the basis of mutations that cause disease in humans. Mutations in a putative ASF/SF2 binding motif (nucleotides 406–412) reduced PLP 5′ donor site selection, whereas a mutation in a putative SC35 binding motif (nucleotides 382–389) had no effect. UV crosslinking and immunoprecipitation (IP) assays using an antibody to ASF/SF2 showed that the ASF/SF2 protein specifically binds to the ESE (nucleotides 406–412). The single nucleotide mutations that reduced PLP splice site selection greatly diminished ASF/SF2 protein binding to this motif. We next tested the effect of overexpressed ASF/SF2 on PLP 5′splice selection in differentiating oligodendrocytes. ASF/SF2 positively regulates PLP splice site selection in a concentration-dependent manner. Disruption of the putative ASF/SF2 binding site in exon 3B reduced the positive effect of ASF/SF2 on PLP splicing. We conclude that an ESE in exon3B regulates PLP 5′ donor site selection and that ASF/SF2 protein participates in the regulation of PLP alternative splicing in oligodendrocytes. J. Cell. Biochem. 97: 999–1016, 2006.

Key words: proteolipid protein; alternative splicing; exonic splicing enhancer; oligodendrocytes; ASF/SF2

Proteolipid protein 1 (PLP1) is the major intrinsic protein of central nervous system myelin, and it comprises two protein products, PLP and DM20 that originate from the alternative splicing of exon 3 [Nave et al., 1987]. The oligodendrocytes are the myelin producing cells of the central nervous system and express PLP/DM20 in a developmentally regulated fashion. During embryonic development when oligodendrocyte progenitor cells (OPC) are generated in the brain, low levels of DM20 message, and protein are expressed [Stecca et al., 2000]. In the postnatal brain during lineage progression of the oligodendrocytes and myelination, PLP is expressed at high level and becomes the predominant transcript, and protein product with a ratio to DM20 of 3:1 [LeVine et al., 1990; Stecca et al., 2000]. PLP and DM20 transcripts are generated through the alternative selection of two competing 5′ donor sites resulting in the inclusion of 105 nucleotides in the PLP transcript. As a result, the PLP protein contains 35 amino acids in the major intracellular loop that are absent in the DM20 product and that confer unique properties to PLP that are not shared

Grant sponsor: NIH (to GMH, FC); Grant number: 1P20RR020173-01; Grant sponsor: NMSS (to GMH, FC); Grant number: PP0860; Grant sponsor: Health Research Grant PA (FC); Grant number: 01-07-26; Grant sponsor: The Nemours Foundation (to GMH).

*Correspondence to: Franca Cambi, MD, PhD, Department of Neurology, KY Clinic L445, Lexington, KY 40536-0284. E-mail: franca.cambi@uky.edu

Received 21 July 2005; Accepted 19 September 2005
DOI 10.1002/jcb.20692

by DM20 [Gow et al., 1998; Gudz et al., 2002]. A unique function of PLP is also supported by observations that mutations occurring in humans that affect either PLP specific region or PLP specific splicing are associated with axonal degeneration [Garbern et al., 2002; Hobson et al., 2002; Shy et al., 2003]. Therefore, alternative splicing of PLP/DM20 is under developmental regulation during oligodendrocyte differentiation and regulated splicing of PLP plays a critical role in myelin and axon stability [Hobson et al., 2002].

Splice sites flanking alternatively spliced exons are usually weak and their selection is regulated by exonic and intronic enhancers [Stamm et al., 1994; Thompson et al., 2002]. The PLP and DM20 5′ donor sites are both weak, but the PLP site is stronger than the DM20 site [Rogan et al., 2003; Hobson et al., 2005]. Interestingly, the DM20 donor site although weaker than PLP is preferentially utilized by non-myelin cells, whereas the PLP 5′donor site is exclusively utilized in myelin producing cells, oligodendrocytes, and Schwann cells, suggesting an active mechanism of splice site selection. We identified a G-rich element in intron 3 of the *PLP* gene that acts as an intronic splicing enhancer and is necessary for PLP splice site recognition in oligodendrocytes [McCullough and Berget, 1997; Hobson et al., 2002]. Deletion of this element significantly reduces PLP splice site selection in oligodendrocytes, although it does not affect recognition of the DM20 splice site. High level of temporally regulated PLP splicing and PLP accumulation occur only in differentiated oligodendrocytes. It is conceivable that, in addition to the ISE, additional regulatory sequences both intronic and exonic play a role in the regulation of PLP/DM20 alternative splicing and may contribute to the temporal and spatial regulation of PLP splice site selection.

Positive regulatory elements, termed exonic splicing enhancers (ESE) are typically located in alternatively spliced exons and are either purine or pyrimidine rich sequences [Blencowe, 2000]. ESEs are typically degenerate sequences of low complexity 5–7 nucleotides in length [Liu et al., 1998]. They bind to a class of RNA binding proteins, the SR proteins, which contain one to two RNA recognition motifs that confer sequence specificity and a serine-arginine (SR)-rich domain at the C terminus [Hastings and Krainer, 2001]. ASF/SF2 and SC35 are well-characterized members of the family of SR proteins, and participate in both constitutive and regulated splicing via the recognition of distinct binding motifs [Fu et al., 1992; Caceres et al., 1997]. Binding motifs for distinct SR proteins are spatially distributed in some alternatively spliced exons, suggesting differential roles in splice selection [Caceres and Kornblihtt, 2002]. In addition, these sites often are present in clusters, suggesting that multiple copies are necessary for optimal function [Liu et al., 1998]. In alternatively spliced exons, ASF/SF2 was shown to favor the proximal 5′ splice site (i.e., the site that is more downstream and closer to the 3′ acceptor site) in a concentration-dependent fashion, supporting that alternative splicing of some genes may be influenced by modulation of the amount of the SR proteins in specific-cell types during development and differentiation [Ge and Manley, 1990; Zahler et al., 1993]. Other modifications, such as degree of phosphorylation, shuttling between nucleus and cytoplasm, levels of expression, and alternatively spliced forms may all contribute to functional modulation of the activity of these ubiquitous proteins [Caceres et al., 1998; Stamm, 2002].

Mutations in ESEs cause a number of genetic diseases by abolishing the enhancer's function and resulting in missplicing [Cartegni and Krainer, 2002; Wang et al., 2004]. We showed that mutations at the PLP and DM20 splice sites [Hobson et al., 2005] and deletion of an intronic splicing enhancer of PLP splice selection are associated with Pelizaeus–Merzbacher disease (PMD) in humans [Hobson et al., 2002]. To date, studies on mutations associated with PMD that occur at PLP ESEs and disrupt PLP alternative splicing have not yet been reported.

In this study, we sought to investigate whether ESE and SR proteins play a role in PLP alternative splicing regulation in primary oligodendrocytes in vitro. We selected mutations that occur at binding motifs for ASF/SF2 and SC35 in PLP exon 3B and that are associated with PMD in humans. We found that a putative ASF/SF2 binding motif positively regulated PLP specific splice site selection, and we showed that binding of ASF/SF2 protein is drastically diminished by the mutations occurring at this site. To further explore the function of ASF/SF2, we assessed the contribution of ASF/SF2 to PLP alternative splicing by

overexpressing ASF/SF2 in differentiating oligodendrocytes and we tested whether the mutations in the ASF/SF2 binding motif decreases the positive effect of ASF/SF2 on PLP splicing. Finally, we characterized the expression pattern of ASF/SF2 during lineage progression of oligodendrocytes.

MATERIALS AND METHODS

Cell Cultures and Transfections

Mixed primary glial cultures were established from 1-day old Sprague–Dawley rat brain, as previously described [Huang et al., 2002]. Purified OPCs were obtained by shake-off of mixed cultures followed by removal of microglia and immunopanning with antibodies that remove contaminating astrocytes (Ran 2). These oligodendrocyte preparations are >95% pure and were utilized for all transfections experiments [Huang et al., 2002]. An additional selection with A2B5 was used to obtain oligodendrocyte progenitor cells >98% pure, which were utilized in immuocytochemistry studies and Western blot, except when noted in the figure legend. OPCs were expanded in chemically defined medium containing 30% B104 medium and supplemented with human aa-PDGF (10 ng/ml) (R&D Systems, Minneapolis, MN) and b-FGF (20ng/ml) (R&D Systems). For lineage progression studies, OPCs were differentiated in either N1 medium devoid of mitogens or T3 containing medium and harvested 24 and 72 h later, as previously described [Huang et al., 2002]. For transfections, precursors were plated in six-well plates coated with poly-D-ornithine at 7×10^5 cells per well and grown in 30% B104 conditioned media supplemented with 10 ng/ml aa-PDGF and 20 ng/ml b-FGF. The plasmid DNA used for transfection was prepared with the EndoFree™ Plasmid Maxi kit (Qiagen, Valencia, CA) following the manufacturer's instructions. Cells were transfected with plasmid DNA using Qiagen Effectene Transfection Reagents according to the manufacturer's instructions (Qiagen). After 6 h, the medium was replaced with fresh growth medium, and 18 h later, the growth medium was replaced with differentiation medium supplemented with T3 (40 ng/ml medium). After 48 h in differentiation medium, the cells were harvested.

The immortalized oligodendroglial precursor cell line (Oli-neu, kind gift of Dr. Trotter) was cultured as described [Jung et al., 1995]. Precursor cells were cultured in SATO medium supplemented with 1% horse serum (GIBCO) and induced to differentiate by addition of dibutyryl cyclic adenosine mono phosphate (1 mM, Sigma) for 7–10 days.

L cells were grown in DMEM containing 10% FBS, seeded in six-well plates at 3×10^5/well and after 24 h were transfected with plasmid DNAs using Qiagen Effectene Transfection Reagents (Qiagen).

In all co-transfection experiments except for the concentration-dependent effects of ASF/SF2 (see below), cells were transfected with 0.5 μg of the PLP splicing construct with 0.5 μg of the SC35 and ASF/SF2 expressing plasmids. Controls were co-transfected with 0.5 μg of PLP splicing construct and 0.5 μg of pcDNA3 plasmid. Dose curve experiments were carried out by co-transfecting 0.5 μg of PLP splicing construct with 0.5–1.5 μg of ASF/SF2 or SC35 expressing plasmids.

Plasmids and RT-PCR Analysis

Mutations were introduced into a previously described minigene splicing construct [Hobson et al., 2002] by site directed mutagenesis using the QuikChange Site-Directed Mutagenesis Kit (Stratagene, La Jolla, CA) according to the manufacturer's instructions. All constructs were verified by automated fluorescent sequence analysis on a Prism 377 DNA Sequencer (Applied Biosystems, Foster City, CA).

Total RNA was extracted using the RNeasy Mini Kit (Qiagen) and was treated with the DNA-free Kit (Ambion, Austin, TX) according to the manufacturer's instructions. Reverse transcription was performed with 1 μg of total RNA using random hexamer primer mixture according to the manufacturers instructions (BD Biosciences, Palo Alto, CA). To amplify the PLP splice product, PCR reactions were carried out with the forward primer III (5′-GTTCCAGAGGCCAACATCAAGCTC-3′) complementary to the PLP exon 3B, and the Cy5-labeled reverse primer IV (5′-CTTCAGCAATATCACGGGTAGCCA-3′) in the *neo* gene sequence (Fig. 1). To amplify both DM20 and PLP splice products together, PCR reactions were carried out using the Cy5-labeled forward primer I (5′-GATGATCTGGACGAAGAGCATCAG-3′) in the *neo* gene sequence and the reverse primer II (5′-TTGCCGCAGATGGTGGTCTTGTAG-3′) complementary to the PLP exon 3A [Hobson et al., 2002]. To amplify both DM20 and PLP

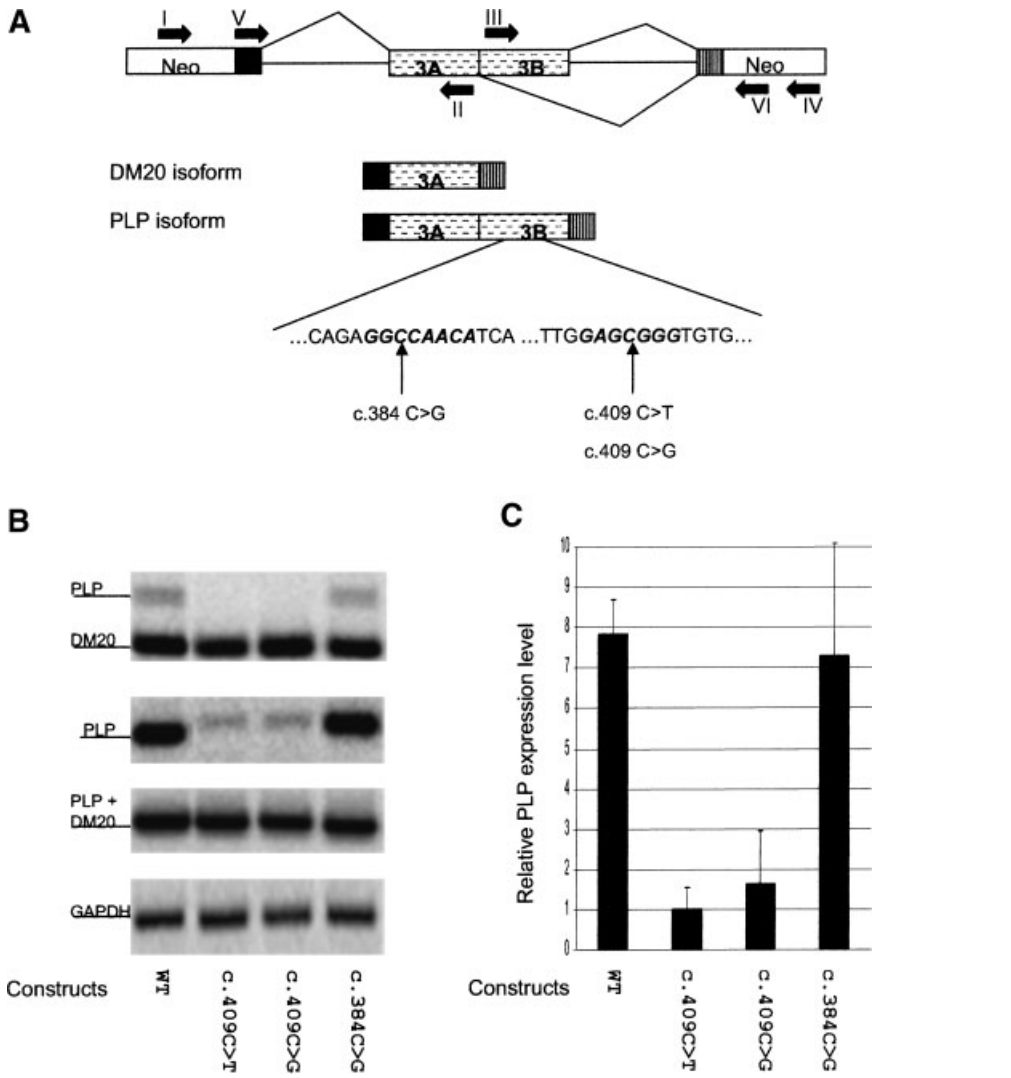

Fig. 1. Effects of single nucleotide mutations in exon 3B on the alternative splicing of PLP. **A**: Schematic representation of the PLP splicing construct used for in vitro transfections, and the alternatively spliced isoforms (not to scale). Arrows show the positions of the primers used for amplification of splicing products derived from the PLP minigene. Primer V and IV amplify both PLP and DM20 splice products as separate bands and are complementary to PLP exon 2 and neomycin sequences, respectively. Primer V and VI (complementary to PLP exon 2 and neomycin sequences, respectively) also amplify both PLP and DM20 splice products as separate bands. Primers III and IV amplify PLP specific product only, while primers II and I amplify the PLP and DM20 as one product. Neo indicates the neomycin gene. The exon 3B alternatively spliced products are shown. Partial sequence of exon 3B with the SC35 and ASF/SF2 binding motifs (bold), and the position of the mutations at c.384C and at c.409C are shown. **B**: RT-PCR analyses of PLP and DM20 splice products derived from PLP minigene constructs transfected into oligodendrocytes, as described in Methods. In order to detect and quantitate a PLP specific product derived from the plasmid containing the 409 mutations, we used 40 cycles of PCR for the amplification of the PLP specific product. WT is the wild-type PLP neo minigene, c.409C > T, c.409C > G, and c.384C > G indicate the PLP neo minigene carrying mutation at nucleotide 409 and 384. The amount of DNA of each transfected plasmid construct is 0.5 μg. Mutations at 409 reduce the amount of PLP specific product by 80%–90%. The mutation at 384 does not reduce the amount of PLP specific product. **C**: Bar graph represents levels of PLP splice product from each construct expressed as the ratio of PLP product to the PLP + DM20 product corrected by the GAPDH signal (mean of four independent experiments ± SD).

splice products simultaneously, PCR reactions were performed using the forward primer V (5′-G-GCACAGAAAAGCTAATTGAGACC-3′) complementary to the PLP exon 2, and the Cy5-labeled reverse primer IV or primer VI (5′-GCCATTTTCCACCATGATATTCGG-3′) in the *neo* gene sequence (Fig. 1). The GAPDH transcript was amplified as the internal control.

To determine the linear range of PCR amplification for each primer set used in this study, a

PCR master mix for each primer set was prepared and divided into 10 aliquots. After 19 PCR cycles, aliquots were removed every 2 cycles, the PCR products were separated on agarose gel, and the band intensity was quantified by a Storm Phosphorimaging System (Molecular Dynamics, Sunnyvale, CA). The linear range of amplification was obtained by plotting cycle number against the band intensity. A cycle number in the middle of the linear range was chosen as the optimal PCR amplification. Our experiments showed that the optimal PCR cycle number for the primer set III and IV (amplification of PLP transcript only), and the primer set I and II (amplification of PLP and DM20 transcripts as a single band) were 35 and 30, respectively (data not shown). These cycle numbers were used for all RT-PCR of PLP splicing products (except where noted in the figure legends). The optimal PCR cycle number for the amplification of GAPDH transcripts was 25.

PCR reactions were performed with 2 μl of the RT cDNA in ABI3000 (Applied Biosystems) using the following conditions: initial denaturation 94°C for 3 min; 94°C for 20 s, 58°C for 30 s, 72°C for 1 min for the aforementioned optimal number of cycles (except where noted in the figure legends), and final extension at 72°C for 7 min. The PCR products were separated on 1.5% agarose gel (Invitrogen, Carslab, CA), and band intensities were quantitated on a Storm Phosphorimaging System (Molecular Dynamics). Relative PLP levels were calculated by dividing the PLP only signal from each transfected construct by the PLP + DM20 signal corrected by the GAPDH. The data were obtained in three to six independent experiments using separate oligodendrocyte preparations and are expressed as the mean ± SD. The statistical significance was assessed with Student *t*-test.

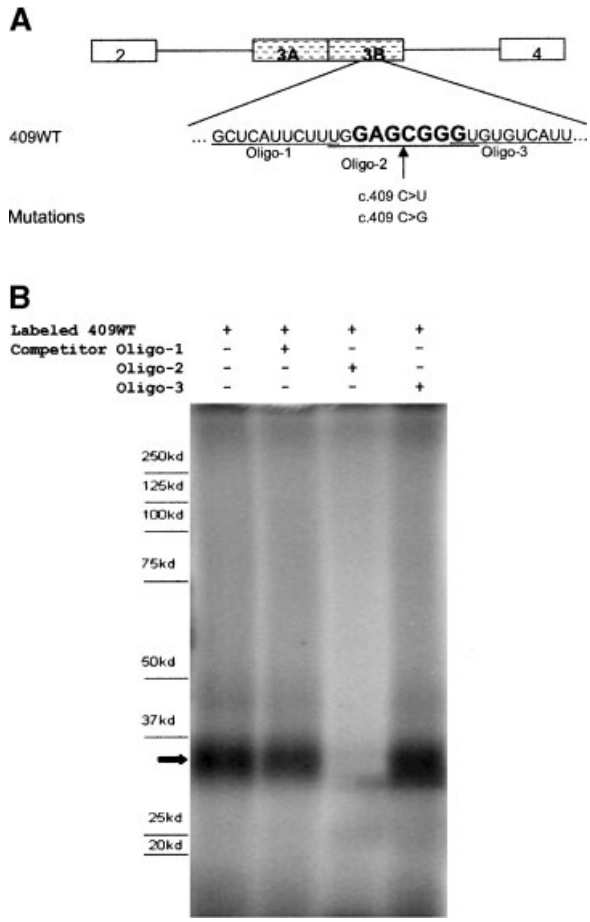

Fig. 2. Sequence specificity of binding determined by UV crosslinking of purified recombinant ASF/SF2. **A**: Sequence of the wild-type RNA probe 409WT. The putative ASF/SF2 binding motif is in enlarged and bold case. Underlined are the three RNA oligos used as the competitors in the competition analysis. The single nucleotide mutations (C > U and C > G) are indicated below the arrow. **B**: UV crosslinking analysis of the ^{32}P labeled wild-type RNA probe 409WT with purified recombinant ASF/SF2 protein with and without cold competitors. Purified recombinant ASF/SF2 (0.2 μg) was used in UV crosslinking reactions. The molar ratio of cold competitive/labeled RNA was 25. The crosslinked complexes were separated on 8% SDS–PAGE and visualized by PhosphorImager. Protein markers are shown on the left. The arrow points to the putative crosslinked ASF/SF2 protein.

UV Crosslinking and Immunoprecipitation Assays

HPLC purified synthetic RNA oligonucleotides were purchased from Integrated DNA Technologies, Inc., 409WT is a 28 bp oligoribonucleotide that contains the natural PLP sequences spanning the ASF/SF2 binding motif (5′-GCUCAUUCUUUGGAGCGGGUGUGUCAUU-3′, underlined is the putative ASF/SF2 binding motif) while 409C > U and 409C > G are RNA oligonucleotides in which the 409C (in bold) was mutated to U and G, respectively (Fig. 2A). Oligo-1 (5′-GCUCAUUCUU-3′), Oligo-2 (5′-UGGAGCGGGU-3′), and Oligo-3 (5′-GUGUGUCAUU-3′) are oligoribonucleotides that span partially overlapping 10 nucleotide sequences from 5′ to 3′ of 409WT (Fig. 2A). Synthetic RNA templates were phosphorylated with [γ-^{32}P] ATP (Amersham Biosciences, Piscataway, NJ) using T4 polynucleotide kinase (Promega, Madison, WI). Nuclear extracts were prepared from differentiated Oli-neu cells by using the NEP kit

according to the manufacturer's instructions (Pierce, Rockford, IL). HeLa cell extracts were prepared as described [McCullough and Berget, 2000].

For UV cross linking ^{32}P labeled synthetic oligoribonucleotides (~50,000 cpm) were incubated with nuclear extracts in buffer containing 4 mM creatine, 2 mM ATP, 1.5 mM $MgCl_2$, 1.2 mM DTT for 10 min at 30°C, and heparin was added and the reactions were exposed to 254 nm UV light with a Spectronics XL-1000 UV crosslinker at a setting of 1.8 J/cm^2 on ice (about 10 min). Samples were subject to SDS–PAGE analysis and visualized by PhosphorImager (Molecular Dynamics).

For immunoprecipitation (IP) analysis, UV crosslinked nuclear extracts (~120 μg proteins) were diluted into 1,000 μl with IP buffer [50 mM Tris-HCL, pH 8.0; 150 mM NaCl; 0.1% Nonidet P-40; 100 μl Halt Protease Inhibitor Cocktail (Pierce)] and 10 μl (5μg) of either anti-ASF/SF2 antibody (Zymed Laboratories, San Francisco, CA) or 5 μg of control mouse IgG (Jackson ImmunoResearch Laboratories) were added, and incubated at 4°C with rocking for 3 h. Protein A-Agarose beads (100 μl, Santa Cruz Biotechnology, Santa Cruz, CA) were added to the IP mixtures, and after overnight incubation at 4°C with rocking, the samples were washed six times with IP buffer and heated at 95°C for 3 min in SDS–PAGE loading buffer. The immunoprecipitated proteins were separated by 8%–10% SDS–PAGE and visualized by PhosphorImager.

Immunocytochemistry and Western Blot Analysis

Cells were grown on glass coverslips, fixed in 4% paraformaldehyde for 10 min, reacted with monoclonal antibodies directed to SC35 (ATCC, mouse hybridoma CRL-2031) and ASF/SF2 (Zymed, mouse monoclonal ASF/SF2 clone 102) diluted 1:150 overnight at RT, followed by either FITC- or rhodamine-conjugated secondary antibody (Jackson ImmunoResearch Laboratories) diluted 1:500 for 30 min at RT and mounted with vectashield mounting medium containing 4,6,-diamino-2-phenolidole (DAPI, Vecta laboratories, Burlingame, CA). Digital images were captured with a Leica DMR fluorescent microscope and analyzed using Leica Confocal software (LCS). Double staining of ASF/SF2 and SC35 with monoclonal antibody A2B5, which recognizes OPCs [Eisenbarth et al., 1979] and O1, which recognizes differentiated oligodendrocytes [Sommer and Schachner, 1981] was performed as follows. Live cells were reacted with either A2B5 or O1 hybridoma supernatant diluted 1:10 in PBS followed by FITC conjugated secondary antibody diluted 1:100. Cells were fixed in 4% paraformaldehyde for 10 min, permeabilized with 0.5% Triton X100 in TBS containing gelatin, goat serum, and BSA for 10 min, and incubated with the ASF/SF2 and SC35 antibody as described above. Coverslips were mounted with vectashield mounting medium containing DAPI. Cells were viewed under Zeiss epifluorescence microscope Axiovert 100TV and images captured with digital image analysis system, Kodak DC 290 digital camera.

Nuclear and cytoplasmic extracts were prepared from OPC and oligodendrocytes using the NEP kit (Pierce) according to manufacturer's instructions [Huang et al., 2002]. Steady-state levels of CNPase, cyclin D1, SC35, ASF/SF2, β-tubulin, and β-actin were determined by Western blot analysis. Nine micrograms and 18 μg from nuclear and cytoplasmic extracts, respectively, were separated by 10% SDS–PAGE, transferred to nitrocellulose membrane (Hybond-ECL, Amersham) and reacted with commercially available antibodies to CNPase (Sternberger, SMI-91), cyclin D1 (Santa Cruz, sc-717), ASF/SF2 (Zymed, mouse monoclonal, ASF/SF2 clone 102), β-tubulin (Sigma T 4026), β-actin (Sigma A 2668) at 1:2,000 dilution, and SC35 (ATCC, mouse hybridoma CRL-2031), at 1:500 dilution followed by HRP-conjugated secondary antibody (Jackson ImmunoResearch Laboratories) diluted 1:5,000 and developed with enhanced chemiluminescence (ECL, Amersham) [Tang et al., 1998].

RESULTS

Mutations in a Putative ASF/SF2 Binding Motif Reduce PLP Specific Splice Site Selection

By using bioinformatics analysis with the ESE finder tool [Cartegni et al., 2003], we identified several putative ASF/SF2 binding motifs, most of which are clustered towards the 5′ portion of exon 3B and in part are overlapping with SC35 binding motifs (data not shown). To identify ESE functionally important in PLP alternative splicing, we selected mutations in exon 3B that were identified in patients diagnosed with PMD and that were found by

ESE finder analysis to occur at ASF/SF2 and SC35 binding motifs (Fig. 1A). ESE finder analysis predicted that mutation c.384C > G eliminates a SC35 site (nt. 382-389, nucleotides were numbered starting from A of the first ATG), while it strengthens an overlapping ASF/SF2 site (nt. 379–385), and mutations c.409C > T and c.409C > G eliminate an ASF/SF2 binding motif (nucleotides 406–412) (Fig. 1A).

We introduced each mutation in a PLP neo minigene splicing construct containing PLP exon 2 through exon 4 inserted in-frame with the bacterial neo gene driven by a Rous sarcoma virus (RSV) promoter [Hobson et al., 2002] and transfected OPCs with wild type and mutated minigene splicing construct. Transfected OPCs were differentiated for 72 h, total RNA was extracted, and PLP and DM20 splice products were analyzed by RT-PCR with primers that amplify only plasmid-derived PLP and DM20 splice products (Fig. 1A). To detect both PLP and DM20 splice products simultaneously, we used a forward primer specific for PLP exon 2 and a reverse primer specific for the neo sequences beyond exon 4 of the mini-gene, thus spanning the alternatively spliced exon 3 to yield both products (Fig. 1A). Quantification of the PLP specific product was obtained by using a primer specific for neo sequences and a primer specific for exon 3B, the PLP specific portion of exon 3 (Fig. 1A). To quantitate both PLP and DM20 transcripts, PCR was carried out with primers specific for neo sequences and for exon 3A common to both PLP and DM20 that produce a single band comprising both PLP and DM20 products (Fig. 1A). Endogenous GAPDH was amplified to ensure that differences in amplified products were not due to the differences in the amount of RNA. To ensure that the oligodendrocytes had differentiated, the endogenous PLP, and DM20 transcripts were analyzed using the same RT reaction with primers specific for PLP exon 2 and 4 sequences that are not contained in the PLP-neo mini-gene (data not shown). As shown in Figure 1B,C, the PLP specific product is significantly reduced (~80%–90%, mean of four independent experiments) by both mutations at nucleotide 409 that eliminate the ASF/SF2 binding site, whereas mutation at nucleotide 384 that eliminates the SC35 binding site did not reduce PLP splicing (mean of four independent experiments). On the basis of these results, we concluded that an enhancer is located in exon 3B at and around 409nt, and that the putative ASF/SF2 binding motif spanning nucleotides 406–412 may contribute to the enhancer function on PLP splice site selection.

Mutations in a Putative ASF/SF2 Binding Motif Eliminate ASF/SF2 Protein Binding

To demonstrate that ASF/SF2 binding motif is critical for the enhancer function, we tested whether the mutations that reduce PLP 5′ donor site selection impair ASF/SF2 binding. We performed biochemical studies of proteins that bind to a synthetic RNA template spanning the ASF/SF2 motif and containing flanking sequences on either side (Fig. 2). RNA templates extend from nt 394 to 421 and contain the putative ASF/SF2 binding motif (nt 406–412) (Fig. 2A), but none of the other ASF/SF2 motifs present in exon 3B. We carried out UV crosslinking experiments using the ^{32}P-labeled wild-type RNA template (409 WT) and a purified recombinant ASF/SF2 protein from baculovirus (ProteinOne, College Park, MD). To determine the sequence specificity of binding, unlabeled 10 bp oligoribonucleotides (Oligo-1, -2 and -3, Fig. 2A) spanning the ASF/SF2 motif and the flanking sequences were added to the reaction mixture before UV crosslinking. As shown in Figure 2B, the ASF/SF2 protein binds to the wild-type RNA template and its binding is competed by Oligo-2 that spans the ASF/SF2 binding motif, but not by oligonucleotides spanning the flanking sequences (Fig. 2B). These results show that purified ASF/SF2 specifically binds to the ESE in a sequence specific fashion.

To demonstrate that ASF/SF2 binds to the ESE in oligodendrocyte nuclear extracts and that the mutations in the ASF/SF2 motif disrupt its binding, we performed IP assays with anti-ASF/SF2 antibody following UV crosslinking of ^{32}P labeled wild type and mutated RNA templates with nuclear extracts prepared from differentiated Oli-neu and HeLa cells. Since both mutations C > U and C > G gave similar results in splicing assays and similarly reduced PLP 5′ donor site selection (Fig. 1B), for the IP studies we used the RNA template containing the 409C > U mutation. A band with the expected electrophoretic mobility for ASF/SF2 (~33 KDa) was precipitated from the UV crosslinked wild-type RNA template 409 WT (Fig. 3A). In contrast, when the crosslinked

409C > U RNA template was immunoprecipitated with ASF/SF2 antibody the band intensity was ~80% lower than that of the wild-type template (Fig. 3A). Considering that U is usually more reactive than C under UV crosslinking conditions [Cartegni and Krainer, 2002], the difference in ASF/SF2 binding affinity between the WT and 409C > U mutant RNA template might even be greater than 80%. The faint bands with molecular weight greater than 70 kDa are non-specific since they were immunoprecipitated by the control mouse IgG (Fig. 3A). Similar results were obtained in UV crosslinking/IP experiments using HeLa cell nuclear extracts (Fig. 3B).

Taken together, UV crosslinking and IP experiments demonstrate that the ASF/SF2 protein specifically binds to the putative ASF/SF2 binding motif between nt 406–412 in PLP exon 3B, and that single nucleotide mutations in this motif that drastically reduce PLP 5′ splice selection substantially decrease ASF/SF2 binding.

Effects of Overexpressed ASF/SF2 and SC35 on PLP Specific Splice Site Selection

Since an ASF/SF2 motif appears to play a role in PLP 5′donor site selection, we reasoned that ASF/SF2 may be an important protein in the regulation of PLP alternative splicing in oligodendrocytes. We assessed the effects of overexpressed ASF/SF2 on PLP alternative splicing and compared it with that of overexpressed SC35 in differentiating oligodendrocytes. We co-transfected oligodendrocytes with plasmids expressing ASF/SF2 and SC35 under the CMV promoter (kind gift of Dr. J. Manley) and the PLP minigene splicing construct [Hobson et al., 2002]. OPCs were transfected with plasmid DNAs and differentiated for 72 h, total RNA was extracted, and PLP and DM20 splice

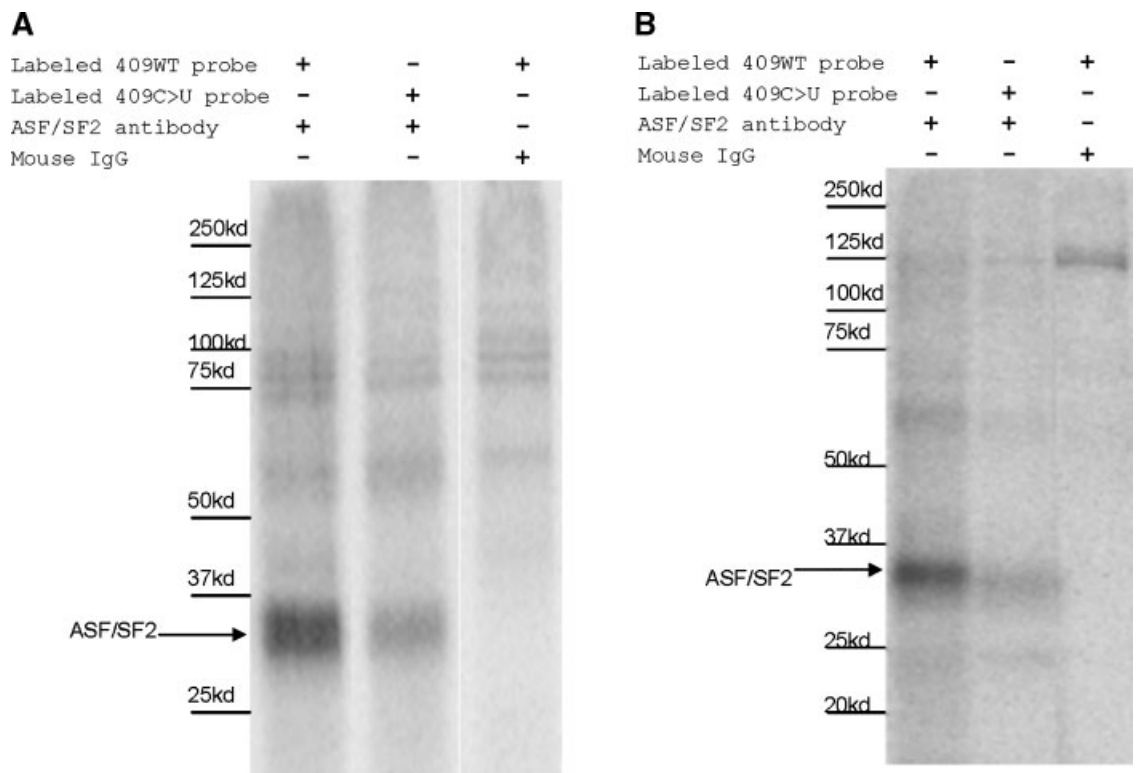

Fig. 3. Immunoprecipitation (IP) of ^{32}P labeled RNA templates UV crosslinked with nuclear extracts. ^{32}P labeled wild-type RNA 409 WT and mutated RNA 409C > U templates were crosslinked with nuclear extracts (120 μg proteins/assay), followed by IP with either anti-ASF/SF2 or mouse IgG (negative control). The immunoprecipitated complexes were separated on 8% (HeLa cells, B) and 10% (Oli-neu cells, A) SDS–PAGE and visualized by PhosphorImager. The experiments were repeated at least two times. **A**: A representative IP experiment using nuclear extracts extracted from differentiated Oli-neu cells. Arrow points to the immunoprecipitated ASF/SF2 protein-RNA complex. Protein markers are shown on the left. **B**: A representative IP experiment using HeLa cell nuclear extracts. Arrow points to the precipitated ASF/SF2 protein-RNA complex. Protein markers are shown on the left.

products were analyzed by RT-PCR with primers, as described above (see Fig. 1A). Endogenous GAPDH was amplified to ensure that differences in amplified products were not the result of differences in amount of RNA. To ensure that the oligodendrocytes had differentiated, the endogenous PLP and DM20 transcripts were analyzed using the same RT reaction with primers specific for PLP exon 2 and 4 sequences that are not contained in the PLP-neo mini-gene (data not shown).

We found that overexpression of ASF/SF2 caused approximately fourfold increase in PLP 5′ donor site selection compared to the control pcDNA3 plasmid (mean of four independent experiments, $P = 0.002$, Fig. 4A,C), whereas overexpression of SC35 induced approximately a twofold increase in PLP splice selection compared to the control pcDNA3 plasmid (mean of three independent experiments, $P = 0.009$, Fig. 4B,D). To assess whether the increase in PLP specific splice site selection induced by ASF/SF2 is concentration dependent, we co-transfected increasing amounts of ASF/SF2 expressing plasmid with the same amount of the PLP splicing minigene into oligodendrocytes. We showed that the PLP specific splice product increased with increasing amount of co-expressed ASF/SF2 (Fig. 5A,B). In contrast, when increasing amounts of SC35 expressing plasmid were co-transfected, we did not detect a concentration-dependent increase in PLP splice products (data not shown).

Both ASF/SF2 and SC35 were previously shown to favor the proximal (i.e., the site closer to the 3′ acceptor site) of two competing 5′ splice sites in alternatively spliced exons [Fu et al., 1992]. To exclude that the stronger effect of ASF/SF2 versus SC35 on PLP splicing in oligodendrocytes is simply the results of the high number of ASF/SF2 binding motifs in exon 3B, we co-transfected either ASF/SF2 or SC35 expressing plasmids with the PLP minigene construct into a fibroblast cell line (L cells), and carried out RT-PCR from RNA prepared 48 h after transfection. We found that both ASF/SF2 and SC35 induced approximately twofold increase in PLP splice site selection (mean of three independent transfections, Fig. 6A,B). Similar results were obtained by co-transfections into HeLa cells (data not shown). These results show that the greater number of ASF/SF2 binding motifs versus SC35 motifs in exon 3B does not induce greater PLP 5′ donor site utilization in non-glial cells and support the hypothesis that the cell specific context influences the function of the ubiquitous ASF/SF2 factor in PLP 5′ donor site selection in oligodendrocytes.

We then tested whether the putative ASF/SF2 binding motif between nt 406 and 412 in exon 3B is functionally relevant in mediating the increase in PLP specific splicing induced by overexpression of ASF/SF2. OPCs were co-transfected with the ASF/SF2 expressing plasmid and either a PLP neo minigene splicing construct that contains the c.409C > T mutation or the wild-type PLP neo splicing construct. PLP splice product was amplified by RT-PCR after 72 h of differentiation and quantitated by PhosphorImager (Fig. 7). The amount of PLP specific product induced by the overexpressed ASF/SF2 from the 409 mutated PLP construct was approximately 50% lower than that from the wild-type PLP construct (Fig. 7, mean of six independent experiments, $P = 0.0003$). These results suggest that disruption of the ASF/SF2 binding motif reduces the positive selection of PLP 5′ donor site induced by overexpressed ASF/SF2.

ASF/SF2 is Expressed Throughout Oligodendrocyte Lineage Progression

Since PLP alternative splicing is associated with oligodendrocyte lineage progression, we next investigated whether the expression and subcellular distribution of ASF/SF2 is modulated during oligodendrocyte lineage progression in vitro. We validated our oligodendrocyte cultures for developmentally regulated PLP alternative splicing and, as previously reported [Sporkel et al., 2002] we detected PLP and DM20 transcripts with ratios of 2:1 and 3:1 in oligodendrocytes differentiated in T3 for 24 and 72 h, respectively (data not shown). Similar ratios were found in oligodendrocytes cultured in N1 medium, although the transcript levels were significantly lower than in T3 medium (data not shown).

Expression and subcellular distribution of ASF/SF2 proteins were determined by Western blot analysis of nuclear and cytoplasmic extracts prepared from OPC, oligodendrocytes cultured in N1 or T3 medium for 24 and 72 h with a monoclonal antibody that reacts to the N-terminus of ASF/SF2 and is independent from its phosphorylation state. To assess cell-cycle arrest, we stained for cyclin D1, which is

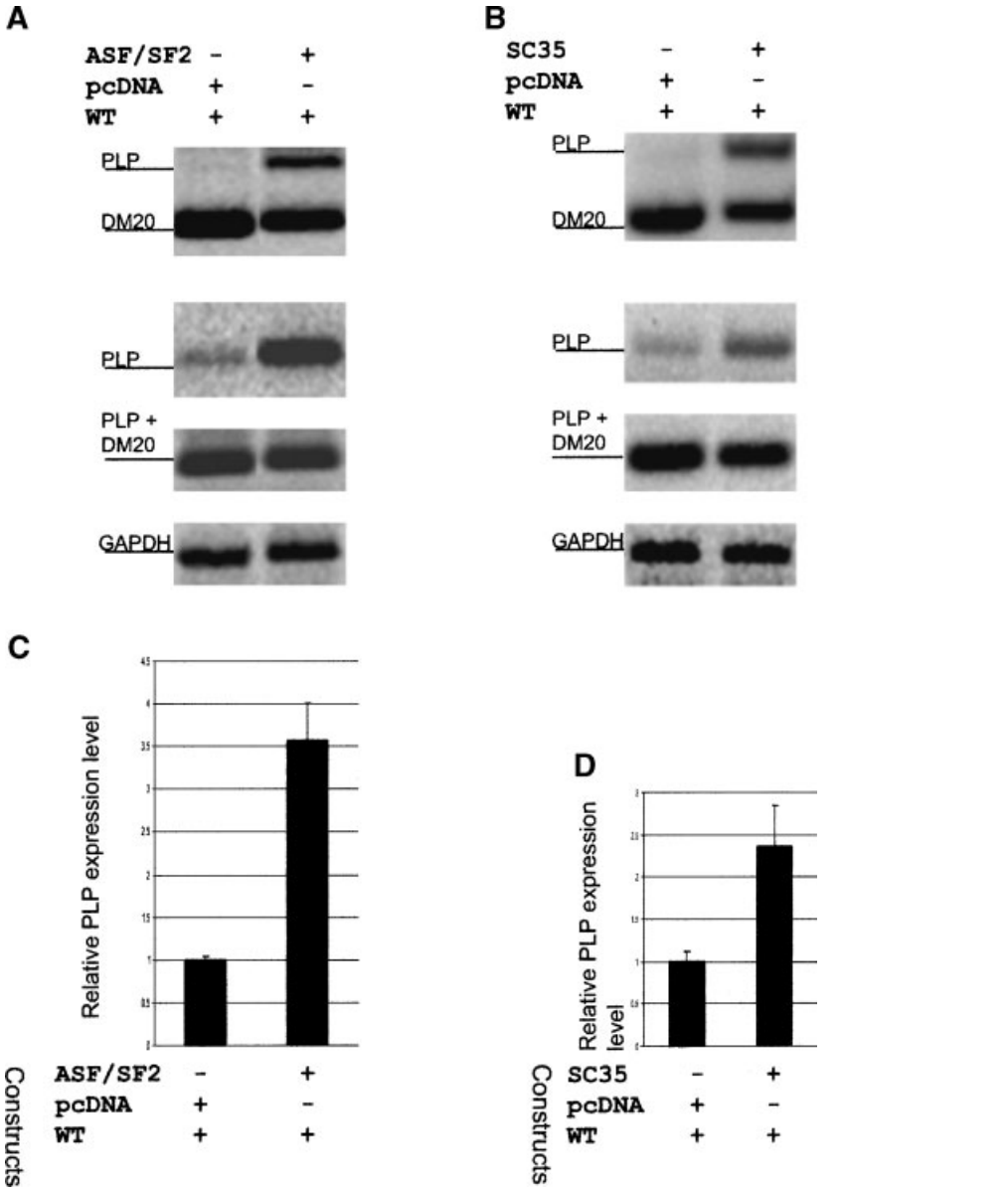

Fig. 4. Effects of overexpressed ASF/SF2 and SC35 on PLP specific splice site selection in oligodendrocytes. **A** and **B**: RT-PCR analyses of PLP and DM20 splice products derived from the PLP minigene construct co-transfected with either ASF/SF2 (A) or SC35 (B) into oligodendrocytes, as described in Methods. WT is the wild-type PLP minigene, pcDNA is the empty plasmid cotransfected to keep constant the total amount of DNA transfected and the total number of CMV promoter copies. ASF/SF2 and SC35 are the plasmids expressing ASF/SF2 and SC35 under the CMV promoter. The DNA amount used for each plasmid construct was 0.5 μg. PLP and DM20 products were PCR amplified as separate bands using 30 cycles with primer set IV and V (A) and V and VI (B). A representative experiment is shown. **C** and **D**: Bar graphs represent the relative level of PLP splice product obtained with co-expressed ASF/SF2 (mean of four independent experiments ± SD) and SC35 (mean of three independent experiments ± SD) plasmid DNAs, respectively. The relative level is the ratio of PLP specific product to the PLP + DM20 product corrected by the GAPDH signal. ASF/SF2 induced approximately fourfold and SC35 induced approximately twofold increase in PLP specific splice product. The increase in PLP specific product is significant with both ASF/SF2 ($P = 0.002$) and with SC35 ($P = 0.009$).

expressed in OPC, and to assess lineage progression, we stained for CNPase, whose expression increases as oligodendrocytes differentiate [Huang et al., 2002]. Antibodies to β-tubulin and to β-actin were used to control for accuracy of protein loading of both nuclear and cytoplasmic extracts, and to assess the purity of the nuclear extract from cytoplasmic contamination. ASF/SF2 was detected in similar abundance in both nuclear and cytoplasmic extracts of OPC and

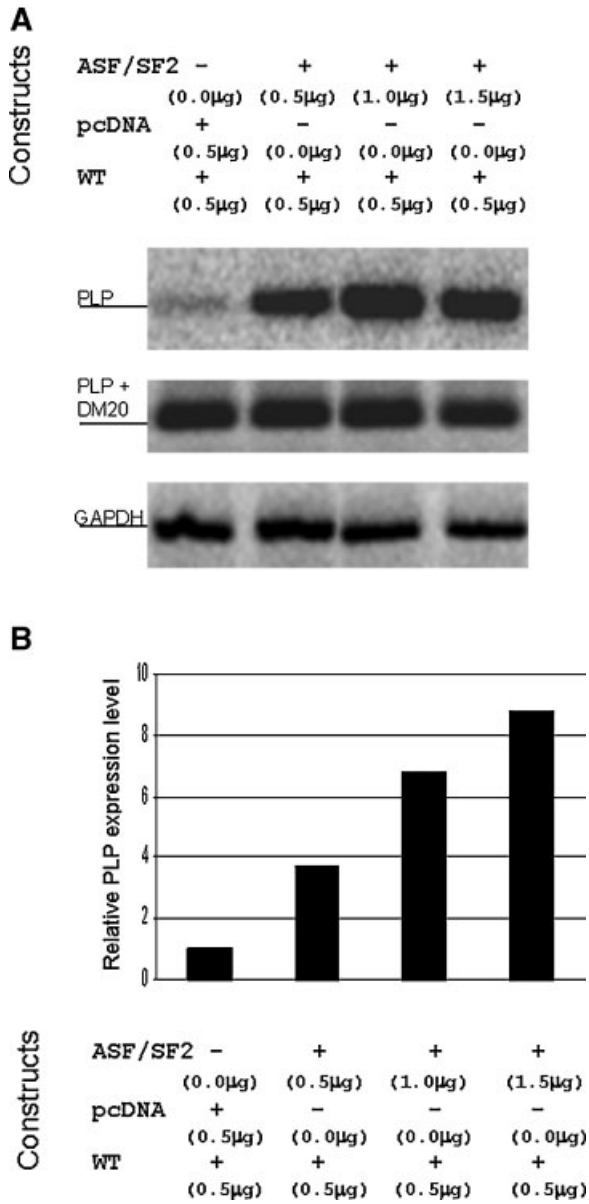

Fig. 5. Increase in PLP splice site selection induced by overexpressed ASF/SF2 is concentration dependent. **A**: RT-PCR analyses of PLP and DM20 splice products derived from the PLP minigene construct co-transfected with increasing amount of ASF/SF2 into oligodendrocytes, as described in Methods. WT is the wild-type PLP minigene, pcDNA is the empty plasmid co-transfected to keep constant the total amount of DNA transfected/dish and the total number of CMV promoter copies/transfection. ASF/SF2 is the plasmid expressing ASF/SF2 under the CMV promoter control. The numbers in brackets show the DNA amounts used in each co-transfection. Increase in PLP specific product is induced in concentration-dependent manner. **B**: Bar graph shows the fold increase of PLP splice product obtained with increasing amount of co-expressed ASF/SF2 plasmid DNA over the control wild-type PLP plasmid set at one (data are averages of two independent experiments).

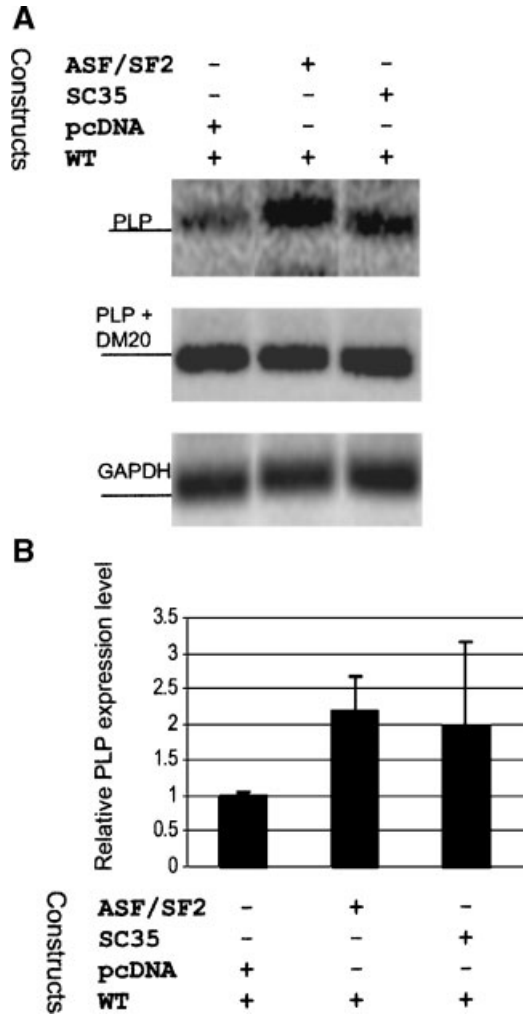

Fig. 6. Effects of overexpressed ASF/SF2 and SC35 on PLP specific splice site selection in L cells. **A**: RT-PCR analyses of PLP and DM20 splice products derived from the PLP minigene construct co-transfected with ASF/SF2 and SC35 into L cells, as described in Methods. WT is the wild-type PLP minigene, pcDNA is the empty plasmid co-transfected to keep constant the total amount of DNA transfected/dish, and the total number of CMV promoter copies/transfection. ASF/SF2 and SC35 are the plasmid expressing ASF/SF2 and SC35 under the CMV promoter control. Increase in PLP specific product induced by both ASF/SF2 and SC35 is of similar magnitude. This is a representative experiment. **B**: Bar graph represents the relative level of PLP splice product obtained with co-expressed ASF/SF2 (mean of three independent experiments ± SD) and SC35 (mean of three independent experiments ± SD) plasmid DNAs, respectively. The relative level is the ratio of PLP specific product to the PLP + DM20 product corrected by the GAPDH signal.

differentiated oligodendrocytes (Fig. 8A). The apparent molecular weight of ASF/SF2 was lower in the cytoplasmic versus nuclear extracts most likely reflecting different degree of phosphorylation (Fig. 8A).

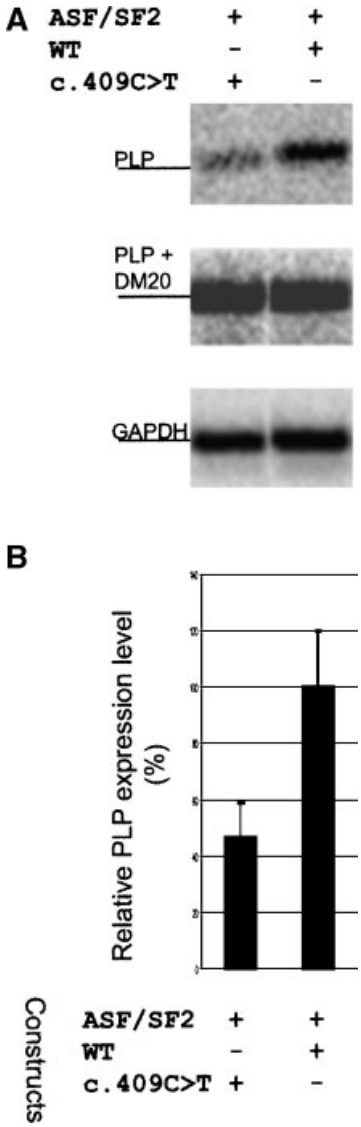

Fig. 7. The c.409C > T mutation reduces the effect of over-expressed ASF/SF2 on PLP splice site selection. **A**: RT-PCR analyses of PLP and DM20 splice products derived from wild type and c.409C > T PLP constructs co-transfected with ASF/SF2 expressing plasmid. Twenty-eight cycles were used to amplify the PLP specific products. **B**: Bar graph shows the PLP splice product induced by co-expression of ASF/SF2 with the 409C > T PLP construct relative to that obtained by co-expressed ASF/SF2 with the wild-type PLP construct (means of six independent experiments ± SD).

To detect ASF/SF2 at the single cell level, we stained OPC and differentiating oligodendrocytes with ASF/SF2 antibody. OPC and oligodendrocytes differentiated for 24 (data not shown) and 72 h stained for ASF/SF2 by immunocytochemistry with three patterns: (1) exclusively cytoplasmic, (2) both nuclear and cytoplasmic, and (3) exclusively nuclear (Fig. 8B). We found a statistically significant decrease in the percentage of doubly stained nuclear and cytoplasmic cells and an increase in the percentage of exclusively nuclear stained cells in differentiated oligodendrocytes for 72 h versus OPC (Fig. 8C, $P = 0.04$ and $P = 0.006$, respectively). To demonstrate the lineage specific expression of ASF/SF2, we analyzed co-expression of ASF/SF2 and oligodendrocyte stage specific markers in OPC and oligodendrocytes differentiated for 72 h, since statistically significant differences in ASF/SF2 expression were detected in oligodendrocytes differentiated for 72 h versus OPC. As shown in Figure 8D, OPC and differentiated oligodendrocytes, recognized with A2B5 and O1 antibody, respectively, express ASF/SF2. Taken together, these results would suggest that greater nuclear localization of ASF/SF2 correlates with oligodendrocyte differentiation.

In contrast to ASF/SF2, SC35, which is non-shuttling SR protein [Cazalla et al., 2002] was detected exclusively in nuclear extracts and appeared to be slightly more abundant in oligodendrocytes differentiated for 72 h, however because of the poor reactivity of the antibody we cannot draw firm conclusions (Fig. 9A). Immunostaining showed that SC35 was present in large and diffuse nuclear clusters in OPC and in oligodendrocytes cultured for 24 h in T3 medium (data not shown), whereas it was distributed in fine speckles in oligodendrocytes differentiated in T3 for 72 h (Fig. 9B). To demonstrate the lineage specific expression of SC35, we analyzed co-expression of SC35 and oligodendrocyte stage specific markers in OPC and oligodendrocytes differentiated for 72 h, since changes in SC35 nuclear pattern were detected in oligodendrocytes differentiated for 72 h versus OPC. As shown in Figure 9C, OPC and differentiated oligodendrocytes recognized with A2B5 and O1 antibody, respectively, express SC35. The change in SC35 clustering may reflect changes in nuclear architecture that may correlate with differentiation of oligodendrocytes.

DISCUSSION

Understanding the regulation of PLP alternative splicing is of critical importance for human disease since disruption of PLP alternative splicing is associated with a neurological disorder, known as PMD [Hobson et al., 2002]. Furthermore, regulation of PLP alternative

splicing is associated with differentiation of oligodendrocytes and coincides with high *PLP* gene transcriptional activation, hence it is intrinsic to the program of oligodendrocyte development ([Timsit et al., 1992; Stecca et al., 2000; Sporkel et al., 2002] and this study). The preferential selection of the PLP 5′ donor site in differentiated oligodendrocytes is controlled at multiple levels. We previously characterized the role of an intronic splicing enhancer, and the contribution of the PLP and DM20 splice site strength in the regulation of PLP alternative splicing [Hobson et al., 2002, 2005].

In the present study, we investigated whether ESEs and their binding factors, the SR proteins play a role in PLP splice site selection. Since the ESE binding motifs are degenerate sequences, putative motifs identified by bioinformatics analysis are not necessarily functionally active [Blencowe, 2000; Cartegni et al., 2003]. Therefore, we examined clinically relevant mutations that occur in PLP exon 3B, and we identified an enhancer of PLP splicing that contains an ASF/SF2 binding motif. Nucleotide changes in the same position in PLP exon 3B were predicted by bioinformatics analysis to abolish the ASF/SF2 motif and were experimentally confirmed to greatly reduce PLP specific splicing and to impair binding of ASF/SF2 to the motif, thus confirming the functional relevance of the ESE and of ASF/SF2 in PLP splice site selection.

A potential role of ASF/SF2 in the regulation of PLP 5′ donor site was further supported by showing that overexpressed ASF/SF2 positively regulates selection of PLP splice site to a greater extent than SC35. Previously, SC35 and ASF/SF2 were shown to favor selection of the proximal (equivalent to the PLP site) of two competing 5′ splice sites [Fu et al., 1992]. Although the increase in PLP splicing induced by ASF/SF2 and to a lesser extent SC35 could represent a general effect of SR proteins, our data would argue that the two SR proteins are not functionally equivalent in the context of *PLP* gene in oligodendrocytes. The increase in PLP selection induced by ASF/SF2 in oligodendrocytes is greater than that induced by SC35 and is concentration dependent. In contrast, SC35 and ASF/SF2 are functionally equivalent in increasing PLP splicing in non-glial cells (L cells). Exon 3B contains eight ASF/SF2 binding motifs, only two ASF/SF2 motifs are located in exon3A, which contains a greater number of SC35 binding sites than exon 3B, suggesting potentially different roles for these two SR proteins in the alternative splicing of PLP and DM20. In the other constitutively spliced PLP exons, ASF/SF2 sites are not as abundant as in exon 3B, in some exons only 1 or 2 sites are present, whereas SC35 sites are more evenly distributed, supporting a role for ASF/SF2 in PLP and DM20 alternative splicing.

Since mutations in the ASF/SF2 binding motif reduce the positive selection of PLP 5′ donor site induced by overexpression of ASF/SF2, the binding motif between nucleotides 406–412 mediates at least in part PLP splice site selection induced by overexpressed ASF/SF2. It is not surprising that the effect of overexpressed ASF/SF2 is only partially reduced by the mutation because the other ASF/SF2 binding motifs present in exon 3B most likely compensate for the loss of this ASF/SF2 motif.

To further establish a relationship between ASF/SF2 and regulation of PLP alternative splicing in differentiating oligodendrocytes, we looked at the expression of ASF/SF2 during maturation of oligodendrocytes. Although the expression of ASF/SF2 did not change during oligodendrocyte maturation in vitro, the function of ASF/SF2 may change in the differentiating oligodendrocytes in response to other functional inputs. Recently, ASF/SF2 was shown to play a critical role in temporally regulated alternative splicing only at specific developmental stages in cardiomyocytes [Xu et al., 2005].

Changes in the degree of ASF/SF2 phosphorylation in differentiating oligodendrocytes can modify the enhancer function [Caceres et al., 1997; Stamm et al., 2005]. Although, we did not assess the phosphorylation of ASF/SF2 as the antibody used for detection reacts to the ASF/SF2 protein independently from its state of phosphorylation, the apparent molecular weight of the ASF/SF2 in the cytoplasmic extracts was lower than in the nuclear extracts suggesting differences in phosphorylation in these two subcellular compartments. ASF/SF2 phosphorylation depends on the activity of a number of kinases, which could be regulated by differentiating signals in oligodendrocytes [Woppmann et al., 1993; Gui et al., 1994; Colwill et al., 1996].

We found that ASF/SF2 was redistributed from the cytoplasm to the nucleus in differentiated oligodendrocytes when PLP 5′ donor site selection increases. Since even small changes in nuclear concentration of splicing factors may

have an impact on alternative splicing, these changes may be of functional significance. A possibility is that ASF/SF2 is counteracted by an inhibitor either a tissue-specific factor or a ubiquitously expressed RNA-binding protein, as it has been shown in other genes [Pollard et al., 2002; Jin et al., 2003] and even small changes in relative levels may have an important functional impact.

The mechanism by which the mutations at nt 409 interfere with ASF/SF2 binding and disrupt PLP 5′ donor site selection remains to be fully investigated. A possible mechanism is that changes in RNA secondary and tertiary structures caused by the mutations affect splicing similarly to the fibronectin gene [Buratti et al., 2004]. We looked at the consequences of the c.409C > T and C > G mutations on the second-

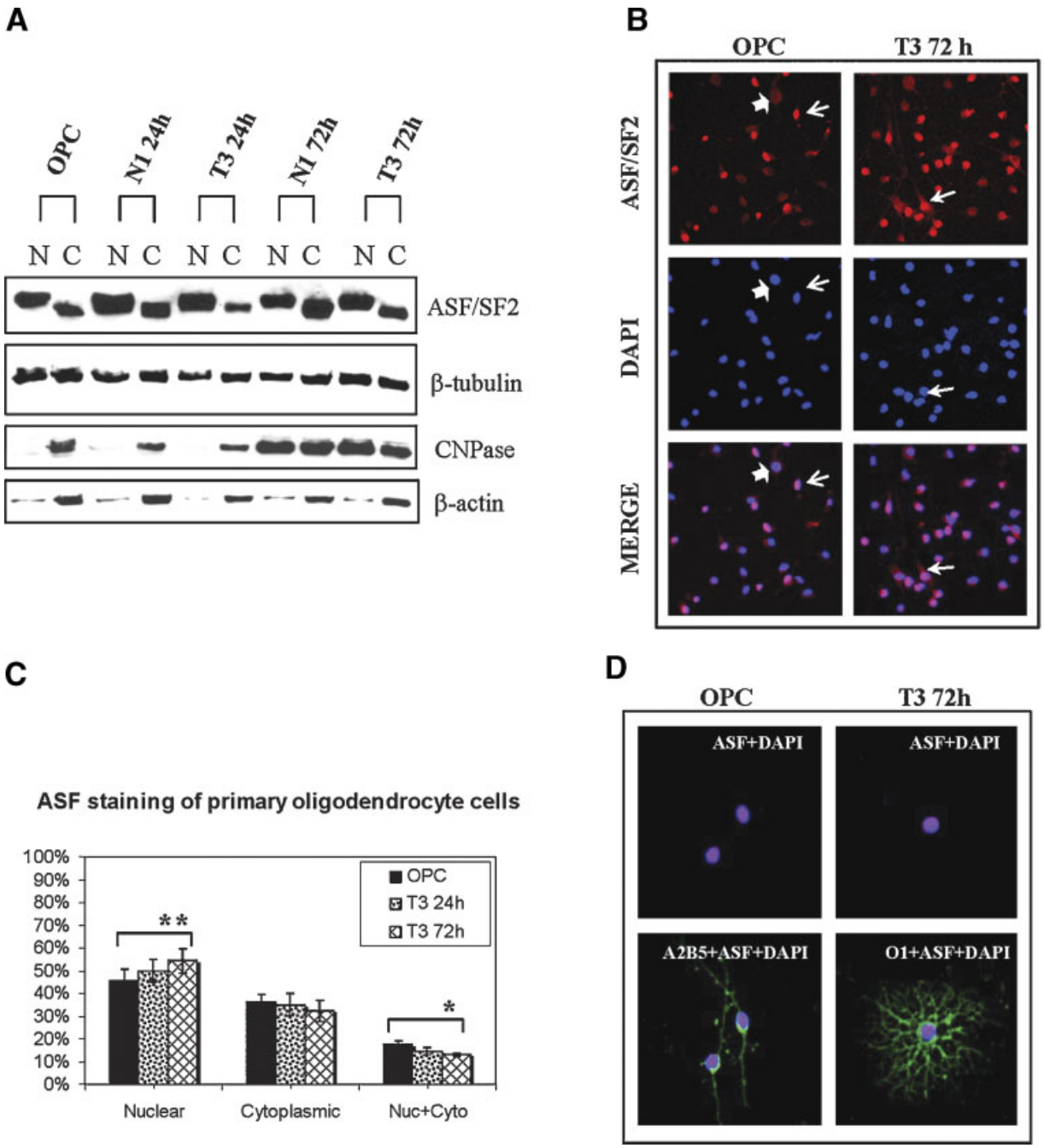

Fig. 8.

ary structure of PLP exon 3B, as predicted with the Mfold program available at http://www.bioinfo.rpi.edu/applications/mfold/old/rna/form1.cgi, [Zuker, 2003]. We found that the sequences between 406 and 412 are part of a stem in a stem-loop structure. Both mutations c.409C > T and c.409C > G modify the stem structure and lead to changes in the secondary structure of the stem and of the adjacent sequences of exon 3B. These changes in secondary structure may alter the interaction of ASF/SF2 with its binding motif and also disrupt binding of other proteins to the flanking sequences.

There are three SC35 binding motifs in exon 3B and we have analyzed the functional relevance of a single SC35 site in which a pathogenic mutation in humans occurred. We show that a mutation in this site predicted to eliminate the motif does not have an effect on PLP splicing. This finding suggests that this SC35 binding motif is not functionally relevant to PLP splicing. However, since the mutation is predicted to strengthen an overlapping ASF/SF2 motif, the latter may compensate for the loss of the SC35 binding motif. The expression levels of SC35 in differentiating oligodendrocytes appear to increase but the levels could not be quantified because of poor reactivity of the antibody in Western blots. SC35 is localized in fine speckles in differentiated oligodendrocytes most likely representing storage centers from which factors can be mobilized in response to stimuli [Lamond and Spector, 2003]. Whether the change in SC35 nuclear distribution in differentiated oligodendrocytes has a functional relevance in *PLP* gene splicing is an intriguing possibility that remains to be explored.

An important contribution of this work is that it provides evidence for the first time that missense mutations in the PLP coding sequences may affect the function of exonic regulatory elements. Assuming that the mutations at nucleotide 409 reduce PLP specific splicing, this would lead to a reduced synthesis of PLP protein carrying the missense mutation, potentially decreasing deleterious consequences of the mutation at the protein level. It is well documented that mutations in the same domain of PLP may lead to phenotypes of different severity through several molecular mechanisms acting at the protein level (review, [Southwood et al., 2002]. Our findings would suggest another possible mechanism by which mutations in the same region of the PLP protein may lead to different phenotypes, depending on whether they impair splicing regulation.

In summary, our results show that ASF/SF2 plays a role in the selection of PLP splicing in differentiating oligodendrocytes and that mutations in an exonic enhancer containing a putative ASF/SF2 binding motif reduce significantly PLP splice site selection and disrupt ASF/SF2 protein binding to the enhancer. Future studies will investigate the mechanisms by which this motif and ASF/SF2 contribute to

Fig. 8. Analysis of ASF/SF2 expression and subcellular distribution in differentiating oligodendrocytes. **A**: Nuclear (N) and cytoplasmic (C) extracts were prepared from OPC and oligodendrocytes cultured in N1 and T3 containing media for 24 and 72 h (N1 24 h, T3 24 h, N1 72 h, and T3 72 h). Proteins were separated in 10% PAGE and transferred to membranes that were probed with antibodies to ASF/SF2, CNPase, β-tubulin, and β-actin. ASF/SF2 was detected in both nuclear and cytoplasmic extracts in OPC, N1 24 h, T3 24 h, and N1 24 h and T3, 72 h. The apparent molecular weight of the band detected in the cytoplasmic extracts is generally lower than that detected in nuclear extracts and it may reflect differences in phosphorylation between nucleus and cytoplasm. CNPase is mostly detected at 24 h in both N1 and T3, and increases in N1 and T3 72 h. CNPase was detected in small amount in the OPC as in this set of experiments progenitor cells were not immunoselected with A2B5 after removal of astrocytes and microglia. This is a representative Western blot from three separate experiments. **B**: OPC and oligodendrocytes differentiated for 72 h were stained with a commercially available monoclonal antibody that recognizes ASF/SF2 and reacted with a Rhodamine conjugated secondary antibody. Nuclei were counterstained with DAPI. Cells were viewed under confocal laser microscopy (Leica TCS NT) at 40× magnification and images were captured and analyzed with LCS. ASF/SF2 is detected in three locations: (1) nucleus (thin arrow), (2) cytoplasm (thick arrow), (3) nucleus + cytoplasm (arrow). **C**: The number of cells with nuclear, cytoplasmic, and nuclear/cytoplasmic ASF/SF2 staining was counted in OPC, T3 24 h, and T3 72 h (total 600 cells/condition). Bar graph represents percentage ± SD for each localization. Reduction in ASF/SF2 nuclear + cytoplasmic and increase in ASF/SF2 nuclear in oligodendrocytes in T3 for 72 h versus OPC were statistically significant, $^{**}P = 0.006$, $^{*}P = 0.04$, respectively. **D**: OPC were co-stained with A2B5 antibody followed by FITC conjugated secondary antibody and with ASF/SF2 antibody followed by Texas Red conjugated secondary antibody. Oligodendrocytes differentiated for 72 h were costained with O1 antibody followed by FITC conjugated secondary antibody and ASF/SF2 antibody followed by Texas Red secondary antibody. Nuclei were counterstained with DAPI. Cells were viewed under Zeiss epifluorescence microscope Axiovert 100TV at 40× magnification and digital images were captured Kodak DC 290 digital camera. [Color figure can be viewed in the online issue, which is available at www.interscience.wiley.com.]

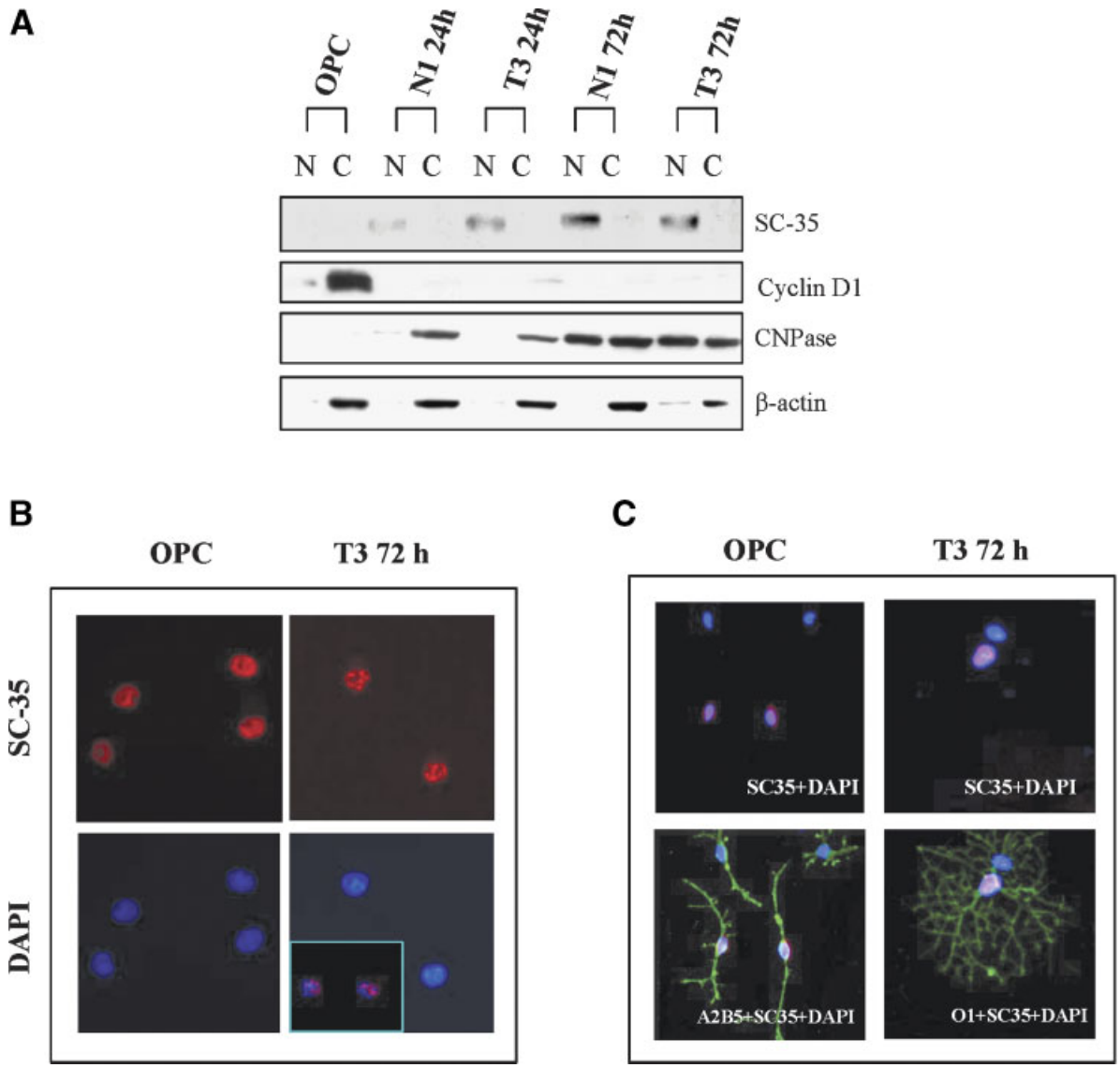

Fig. 9. Analysis of SC35 expression and subcellular distribution in differentiating oligodendrocytes. **A**: Nuclear (N) and cytoplasmic (C) extracts were prepared from OPC and oligodendrocytes cultured in N1 and T3 containing media for 24 and 72 h (N1 24 h, T3 24 h, N1 72 h, and T3 72 h). Proteins were separated in 10% PAGE and transferred to membranes that were probed with SC35, cyclin D1, CNPase, and β-actin. SC35 is detected only in the nucleus of differentiating oligodendrocytes T3 24 h, and N1 24 h and 72 h. We consistently detected only a faint band, possibly due to poor reactivity of the antibody in Western blots. Cyclin D1, a marker of cell proliferation is detected only in dividing OPC. CNPase, a marker of differentiating oligodendrocytes is detected in oligodendrocytes after 24 h in both N1 and T3, and increases after 72 h in N1 and T3. This is a representative Western blot from three separate experiments. **B**: OPC and oligodendrocytes differentiated for 72 h were stained with a commercially available monoclonal antibody that recognizes SC35 and reacted with a Rhodamine conjugated secondary antibody. Nuclei were counterstained with DAPI. Cells were viewed under confocal laser microscopy (Leica TCS NT) at 60× magnification and images were captured and analyzed with Leica Confocal Software(LCS). Inset represents the merged SC35 and DAPI images. SC35 is localized in fine speckles in oligodendrocytes differentiated for 72 h, whereas it is in large and diffuse clumps in OPC. **C**: OPC were co-stained with A2B5 followed by FITC conjugated secondary antibody and with SC35 antibody followed by Texas Red conjugated secondary antibody. Oligodendrocytes differentiated for 72 h were costained with O1 antibody followed by FITC conjugated secondary antibody and SC35 antibody followed by Texas Red secondary antibody. Nuclei were counterstained with DAPI. Cells were viewed under Zeiss epifluorescence microscope Axiovert 100TV at 40× magnification and digital images were captured Kodak DC 290 digital camera. [Color figure can be viewed in the online issue, which is available at www.interscience.wiley.com.]

PLP specific splicing in the context of oligodendrocyte differentiation.

REFERENCES

Blencowe BJ. 2000. Exonic splicing enhancers: Mechanism of action, diversity and role in human genetic diseases. Trends Biochem Sci 25:106–110.

Buratti E, Muro AF, Giombi M, Gherbassi D, Iaconcig A, Baralle FE. 2004. RNA folding affects the recruitment of SR proteins by mouse and human polypurinic enhancer elements in the fibronectin EDA exon. Mol Cell Biol 24: 1387–1400.

Caceres JF, Kornblihtt AR. 2002. Alternative splicing: Multiple control mechanisms and involvement in human disease. Trends Genet 18:186–193.

Caceres JF, Misteli T, Screaton GR, Spector DL, Krainer AR. 1997. Role of the modular domains of SR proteins in subnuclear localization and alternative splicing specificity. J Cell Biol 138:225–238.

Caceres JF, Screaton GR, Krainer AR. 1998. A specific subset of SR proteins shuttles continuously between the nucleus and the cytoplasm. Genes Dev 12:55–66.

Cartegni L, Krainer AR. 2002. Disruption of an SF2/ASF-dependent exonic splicing enhancer in SMN2 causes spinal muscular atrophy in the absence of SMN1. Nat Genet 30:377–384.

Cartegni L, Wang J, Zhu Z, Zhang MQ, Krainer AR. 2003. ESEfinder: A web resource to identify exonic splicing enhancers. Nucleic Acids Res 31:3568–3571.

Cazalla D, Zhu J, Manche L, Huber E, Krainer AR, Caceres JF. 2002. Nuclear export and retention signals in the RS domain of SR proteins. Mol Cell Biol 22:6871–6882.

Colwill K, Feng LL, Yeakley JM, Gish GD, Caceres JF, Pawson T, Fu XD. 1996. SRPK1 and Clk/Sty protein kinases show distinct substrate specificities for serine/arginine-rich splicing factors. J Biol Chem 271:24569–24575.

Eisenbarth GS, Walsh FS, Nirenberg M. 1979. Monoclonal antibody to a plasma membrane antigen of neurons. Proc Natl Acad Sci USA 76:4913–4917.

Fu XD, Mayeda A, Maniatis T, Krainer AR. 1992. General splicing factors SF2 and SC35 have equivalent activities in vitro, and both affect alternative 5′ and 3′ splice site selection. Proc Natl Acad Sci USA 89:11224–11228.

Garbern JY, Yool DA, Moore GJ, Wilds IB, Faulk MW, Klugmann M, Nave KA, Sistermans EA, van der Knaap MS, Bird TD, Shy ME, Kamholz JA, Griffiths IR. 2002. Patients lacking the major CNS myelin protein, proteolipid protein 1, develop length-dependent axonal degeneration in the absence of demyelination and inflammation. Brain 125:551–561.

Ge H, Manley JL. 1990. A protein factor, ASF, controls cell-specific alternative splicing of SV40 early pre-mRNA in vitro. Cell 62:25–34.

Gow A, Southwood CM, Lazzarini RA. 1998. Disrupted proteolipid protein trafficking results in oligodendrocyte apoptosis in an animal model of Pelizaeus–Merzbacher disease. J Cell Biol 140:925–934.

Gudz TI, Schneider TE, Haas TA, Macklin WB. 2002. Myelin proteolipid protein forms a complex with integrins and may participate in integrin receptor signaling in oligodendrocytes. J Neurosci 22:7398–7407.

Gui JF, Tronchere H, Chandler SD, Fu XD. 1994. Purification and characterization of a kinase specific for the serine- and arginine-rich pre-mRNA splicing factors. Proc Natl Acad Sci USA 91:10824–10828.

Hastings ML, Krainer AR. 2001. Pre-mRNA splicing in the new millennium. Curr Opin Cell Biol 13:302–309.

Hobson GM, Huang Z, Sperle K, Stabley DL, Marks HG, Cambi F. 2002. A PLP splicing abnormality is associated with an unusual presentation of PMD. Ann Neurol 52: 477–488.

Hobson G, Huang Z, Sperle K, Sistermans E, Rogan P, Garbern J, Kolodny E, Naidu S, Cambi F. 2005. Analysis of the contribution of splice site strength in the regulation of proteolipid protein and DM20 alternative splicing in differentiating oligodendrocytes in vitro. HUMU (in press).

Huang Z, Tang XM, Cambi F. 2002. Down-regulation of the retinoblastoma protein (rb) is associated with rat oligodendrocyte differentiation. Mol Cell Neurosci 19:250–262.

Jin Y, Suzuki H, Maegawa S, Endo H, Sugano S, Hashimoto K, Yasuda K, Inoue K. 2003. A vertebrate RNA-binding protein Fox-1 regulates tissue-specific splicing via the pentanucleotide GCAUG. EMBO J 22: 905–912.

Jung M, Kramer E, Grzenkowski M, Tang K, Blakemore W, Aguzzi A, Khazaie K, Chlichlia K, von Blankenfeld G, Kettenmann H. 1995. Lines of murine oligodendroglial precursor cells immortalized by an activated neu tyrosine kinase show distinct degrees of interaction with axons in vitro and vivo. Eur J Neurosci 7:1245–1265.

Lamond AI, Spector DL. 2003. Nuclear speckles: A model for nuclear organelles. Nat Rev Mol Cell Biol 4:605–612.

LeVine SM, Wong D, Macklin WB. 1990. Developmental expression of proteolipid protein and DM20 mRNAs and proteins in the rat brain. Dev Neurosci 12:235–250.

Liu HX, Zhang M, Krainer AR. 1998. Identification of functional exonic splicing enhancer motifs recognized by individual SR proteins. Genes Dev 12:1998–2012.

McCullough AJ, Berget SM. 1997. G triplets located throughout a class of small vertebrate introns enforce intron borders and regulate splice site selection. Mol Cell Biol 17:4562–4571.

McCullough AJ, Berget SM. 2000. An intronic splicing enhancer binds U1 snRNPs to enhance splicing and select 5′ splice sites. Mol Cell Biol 20:9225–9235.

Nave KA, Lai C, Bloom FE, Milner RJ. 1987. Splice site selection in the proteolipid protein (PLP) gene transcript and primary structure of the DM-20 protein of central nervous system myelin. Proc Natl Acad Sci USA 84: 5665–5669.

Pollard AJ, Krainer AR, Robson SC, Europe-Finner GN. 2002. Alternative splicing of the adenylyl cyclase stimulatory G-protein G alpha(s) is regulated by SF2/ASF and heterogeneous nuclear ribonucleoprotein A1 (hnRNPA1) and involves the use of an unusual TG 3′-splice Site. J Biol Chem 277:15241–15251.

Rogan PK, Svojanovsky S, Leeder JS. 2003. Information theory-based analysis of CYP2C19, CYP2D6 and CYP3A5 splicing mutations. Pharmacogenetics 13:207–218.

Shy ME, Hobson G, Jain M, Boespflug-Tanguy O, Garbern J, Sperle K, Li W, Gow A, Rodriguez D, Bertini E,

Mancias P, Krajewski K, Lewis R, Kamholz J. 2003. Schwann cell expression of PLP1 but not DM20 is necessary to prevent neuropathy. Ann Neurol 53:354–365.

Sommer I, Schachner M. 1981. Monoclonal antibodies (O1 to O4) to oligodendrocyte cell surfaces: An immunocytological study in the central nervous system. Dev Biol 83: 311–327.

Southwood CM, Garbern J, Jiang W, Gow A. 2002. The unfolded protein response modulates disease severity in Pelizaeus–Merzbacher disease. Neuron 36:585–596.

Sporkel O, Uschkureit T, Bussow H, Stoffel W. 2002. Oligodendrocytes expressing exclusively the DM20 isoform of the proteolipid protein gene: Myelination and development. Glia 37:19–30.

Stamm S. 2002. Signals and their transduction pathways regulating alternative splicing: A new dimension of the human genome. Hum Mol Genet 11:2409–416.

Stamm S, Zhang MQ, Marr TG, Helfman DM. 1994. A sequence compilation and comparison of exons that are alternatively spliced in neurons. Nucleic Acids Res 22:1515–1526.

Stamm S, Ben-Ari S, Rafalska I, Tang Y, Zhang Z, Toiber D, Thanaraj TA, Soreq H. 2005. Function of alternative splicing. Gene 344:1–20.

Stecca B, Southwood CM, Gragerov A, Kelley KA, Friedrich VL ,Jr., Gow A. 2000. The evolution of lipophilin genes from invertebrates to tetrapods: DM-20 cannot replace proteolipid protein in CNS myelin. J Neurosci 20:4002–4010.

Tang XM, Strocchi P, Cambi F. 1998. Changes in the activity of cdk2 and cdk5 accompany differentiation of rat primary oligodendrocytes. J Cell Biochem 68:128–137.

Thompson TE, Rogan PK, Risinger JI, Taylor JA. 2002. Splice variants but not mutations of DNA polymerase beta are common in bladder cancer. Cancer Res 62:3251–3256.

Timsit S, Sinoway MP, Levy L, Allinquant B, Stempak J, Staugaitis SM, Colman DR. 1992. The DM20 protein of myelin: Intracellular and surface expression patterns in transfectants. J Neurochem 58:1936–1942.

Wang J, Gao QS, Wang Y, Lafyatis R, Stamm S, Andreadis A. 2004. Tau exon 10, whose missplicing causes frontotemporal dementia, is regulated by an intricate interplay of cis elements and trans factors. J Neurochem 88:1078–1090.

Woppmann A, Will CL, Kornstadt U, Zuo P, Manley JL, Luhrmann R. 1993. Identification of an snRNP-associated kinase activity that phosphorylates arginine/serine rich domains typical of splicing factors. Nucleic Acids Res 21:2815–2822.

Xu X, Yang D, Ding JH, Wang W, Chu PH, Dalton ND, Wang HY, Bermingham JR, Jr., Ye Z, Liu F, Rosenfeld MG, Manley JL, Ross J, Jr., Chen J, Xiao RP, Cheng H, Fu XD. 2005. ASF/SF2-regulated CaMKIIdelta alternative splicing temporally reprograms excitation-contraction coupling in cardiac muscle. Cell 120:59–72.

Zahler AM, Neugebauer KM, Stolk JA, Roth MB. 1993. Human SR proteins and isolation of a cDNA encoding SRp75. Mol Cell Biol 13:4023–4028.

Zuker M. 2003. Mfold web server for nucleic acid folding and hybridization prediction. Nucleic Acids Res 31:3406–3415.